

## APPARENT RESISTIVITY IN THE PRESENCE OF WELL CASINGS<sup>1</sup>

F.N. TROFIMENKOFF<sup>2</sup>, R.H. JOHNSTON<sup>2</sup> and J.W. HASLETT<sup>2</sup>

### ABSTRACT

The effect of embedded conductors such as oil and gas well casings on apparent resistivity measurements on the earth's surface is of interest in geophysical exploration directed to hydrocarbon detection. In this paper, a relatively simple and computationally efficient method of analysis is presented to determine the apparent resistivity error caused by the presence of perfect conductors embedded vertically into the earth. The conductors may be of arbitrary length. The well casing is treated mathematically as a perfectly conducting prolate ellipsoid embedded in an infinite earth, and the potential to which it rises in the presence of a point current source is determined by using the reciprocity principle. The potential in the vicinity of the ellipsoid and the point source is then obtained by modelling the ellipsoid by short line current sources and obtaining the values of these sources by a matrix inversion. This is equivalent to modelling the well casing by using a series of short ellipsoids that overlap by a very small amount at the ends. For practical array geometries and well casing lengths, the numerical results converge when the casing is sectioned into 15 or fewer parts. The currents thus found are equivalent to the currents that actually flow into the different sections of the well casing. A field point potential due to the line current sources and the point current source is then readily found, and can be compared with the undisturbed field point voltage in the absence of the well casing. The ratio of these potentials gives the ratio of the apparent resistivity with and without the casings. Apparent resistivity profiles calculated for Schlumberger and dipole-dipole arrays with adjacent well casings are presented, and results for the Schlumberger array are compared with field measurements in Alberta.

### INTRODUCTION

Recent interest in the use of surface electrical measurements for hydrocarbon exploration has raised new questions regarding possible mechanisms that would explain measurement anomalies<sup>1-4</sup>. It is now generally recognized that the electromagnetic reflection component from subsurface resistivity discontinuities is too small to serve as a reliable indicator<sup>5-7</sup>. The most likely mechanism that could produce observed electrical anom-

alies is the presence of a geochemical halo or plume above the hydrocarbon reservoir<sup>1-3</sup>. These near-surface geochemical plumes may produce resistivity, induced polarization and electromagnetic coupling anomalies whose characteristics depend strongly on the size and depth of the geochemical features.

In order to study the nature of the electrical anomalies experimentally, an obvious choice is to traverse known oil and gas fields. While large anomalies are observed in this way, there is some question as to whether the presence of well casings contributes to a major portion of the observed effects.

This problem has been addressed recently<sup>3</sup> by using numerical techniques to obtain estimates of the effects of well casings on apparent resistivity surveys. These models have been used to interpret measured results over known fields by means of a dipole-dipole transmitter-receiver array configuration. In general, the results have been inconclusive.

This paper presents an accurate and computationally efficient method of determining the effect of well casings on apparent resistivity measurements. Measurements over two large Alberta oil fields are compared in an attempt to resolve the questions of whether existing fields may be used as models for exploration in particular areas, and whether any significant electrical anomalies over hydrocarbon reservoirs are not explained by the presence of well casings.

### MATHEMATICAL FORMULATION

In this work well casings buried vertically in the earth are treated as half-prolate ellipsoids of revolution in an infinite half space, as shown in Figure 1. A single current injection point at some location removed from the well casing is also shown, where it is understood that the current return path is completed at an infinite distance from the well casing. This configuration can be analyzed by using the method of images to consider a

<sup>1</sup>Presented at the Canadian Society of Exploration Geophysicists - Canadian Geophysical Union National Convention, Calgary, Alberta, May 1985.

<sup>2</sup>Department of Electrical Engineering, The University of Calgary, Calgary, Alberta, Canada T2N 1N4

This work was supported by NSERC operating grants number A7776, A7701 and A3382. The authors are grateful to J. Buckle, president of Emtest Resources Ltd., for providing the experimental data.

full ellipsoid in an infinite conducting medium, as shown in Figure 2. For simplicity, the ellipsoid is assumed to have infinite conductivity in the first instance, and to be in perfect electrical contact with the surrounding earth.

If it is assumed that a positive current is injected at the source point, the ellipsoid extracts current from the earth near the injection point and injects current into the earth at its extremities, as shown in Figure 3. If the magnitude of the current that the ellipsoid (or well casing) sinks or generates into the earth along its length can be calculated, the well casing may then be replaced by a series of current sources and sinks. Once this is done, the potential at any other point in the earth may be calculated with respect to infinity. The ratio of the potential at any point to the potential that would arise at that point when the ellipsoid is absent is then the normalized apparent resistivity at that location. The potential of the ellipsoid,  $V_e$ , when current is injected at a distance  $r_1$  from the ellipsoid can be found by using the reciprocity principle. If the source current  $I_s$  is injected

into the ellipsoid, the source point in question takes on a potential  $V_e$  given by<sup>8</sup>

$$V_e = \frac{\rho I_s}{4\pi l_1} \ln \left[ \frac{l_1 + \sqrt{l_1^2 + r_1^2}}{r_1} \right] \quad (1)$$

where  $l_1 = \sqrt{l^2 - (r_d)^2}$ ,  $l$  is the length of the well casing, and  $\rho$  is the resistivity of the earth. The reciprocity principle then states that  $V_e$  is also the potential assumed by the ellipsoid or well casing when current is injected at the source point under consideration.

To calculate the current that each section of the ellipsoid injects into the ground, the length  $2l$  is sectioned into  $M$  elemental line sources, as shown in Figure 4. In general, the potential at any point in a conducting medium due to a line current source  $I$  is given by<sup>8</sup>

$$V_{FP} = \frac{\rho I}{4\pi(z_2 - z_1)} \ln \left[ \frac{(z_2 - z) + \sqrt{(z_2 - z)^2 + r^2}}{(z_1 - z) + \sqrt{(z_1 - z)^2 + r^2}} \right] \quad (2)$$

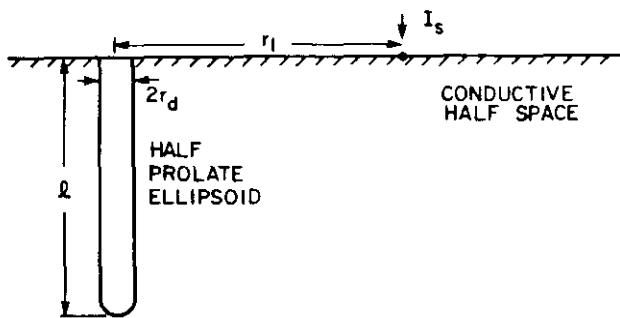


Fig. 1. Model of a well casing in a conductive earth in the presence of an injected current  $I_s$ .

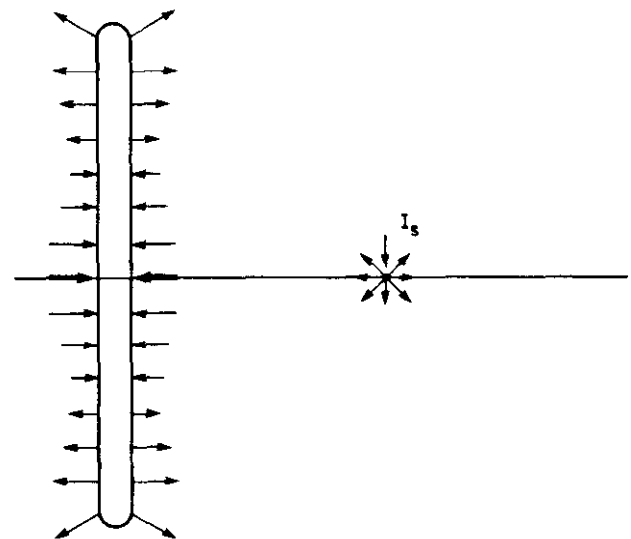


Fig. 3. Well casing current distribution in the presence of an external source  $I_s$ .

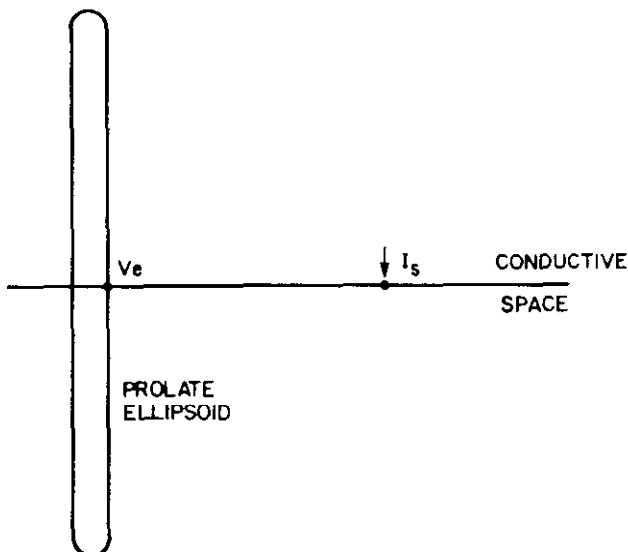


Fig. 2. Analytical model used to represent the well casing embedded in a conductive half space.

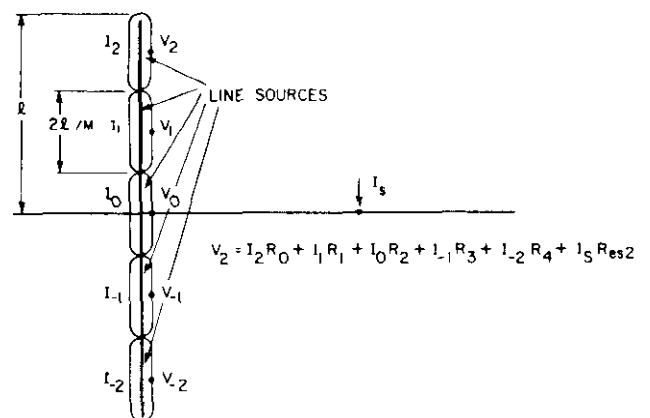


Fig. 4. Sectioned line source model of the embedded casing.

where the dimensions  $z$ ,  $r$ ,  $z_1$  and  $z_2$  are shown in Figure 5. The potential at a distance  $d$  from the line source at any point along the ellipsoid in Figure 4 can then be found by using equation (2), recognizing that each line current source will contribute to the potential at the point of interest. For example, for the uppermost line source in Figure 4 it is possible to write

$$V_2 = R_0 I_2 + R_1 I_1 + R_2 I_0 + R_3 I_{-1} + R_4 I_{-2} + R_{es2} I_s \quad (3)$$

where 
$$R_{es2} = \frac{\rho}{4\pi\sqrt{r_1^2 + (4l/5)^2}}$$

$$R_0 = \frac{\rho}{4\pi l/5} \ln \left[ \frac{2l}{5r_d} \right]$$

and

$$R_p = \frac{5\rho}{8\pi l} \ln \left[ \frac{2p+1}{2p-1} \right] \quad p = 1, 2, 3, 4, \dots, M-1$$

where  $r_d$  is the radius of the well casing, assumed to be much smaller than  $l/5$ . For an arbitrary number of sections,  $M$ , the potential at a radius  $r_d$  from the centre of each line source is given by

$$V_m = R_{esm} I_s + \sum_{n=-N}^N I_n R_{|m-n|} \quad (4)$$

$$R_{esm} = \frac{\rho}{4\pi\sqrt{r_1^2 + (2ml/M)^2}}$$

$$R_0 = \frac{\rho M}{4\pi l} \ln \left[ \frac{2l}{Mr_d} \right],$$

$$R_p = \frac{\rho M}{8\pi l} \ln \left[ \frac{2p+1}{2p-1} \right],$$

where  $p = 1, 2, 3, \dots, N$

and  $N = (M - 1)/2$ .

For  $M$  line sources,  $M$  equations result, and they may be written in matrix form as

$$\begin{bmatrix} V_m \end{bmatrix} - \begin{bmatrix} R_{esm} \end{bmatrix} I_s = \begin{bmatrix} R_0 & R_1 & R_2 & R_3 & R_4 \\ R_1 & R_0 & R_1 & R_2 & R_3 \\ R_2 & R_1 & R_0 & R_1 & R_2 \\ R_3 & R_2 & R_1 & R_0 & R_1 \\ R_4 & R_3 & R_2 & R_1 & R_0 \end{bmatrix} \times \begin{bmatrix} I_n \end{bmatrix} \quad (5)$$

The currents ( $I_n$ ) are set so that all  $V_m$ s become equal to the ellipsoid voltage. The matrix may then be inverted to find the elemental currents that each line source generates or sinks, *i.e.*

$$\begin{bmatrix} I_n \end{bmatrix} = \begin{bmatrix} R^{-1} \end{bmatrix} \times \begin{bmatrix} V_e - R_{esm} I_s \end{bmatrix} \quad (6)$$

The  $R$  matrix is a symmetric Toeplitz matrix and the currents may be found by using the computationally efficient Levinson algorithm. Alternatively, the symmetry of the matrix and the line currents may be noted. It is then clear that the ellipsoid currents are symmetrical around the earth surface plane. Therefore  $I_n = I_{-n}$ , and the top or bottom  $N$  rows of the matrix can be discarded.

It is further possible to combine the columns that correspond to the same absolute current subscript. Writing the matrix in this form gives

$$\begin{bmatrix} V_e - R_{es0} I_s \\ \vdots \\ V_e - R_{esN} I_s \end{bmatrix} = \begin{bmatrix} R_0 & 2R_1 & 2R_2 & \dots & 2R_N \\ R_1 & R_0 + R_2 & R_1 + R_3 & \dots & \vdots \\ R_2 & R_1 + R_3 & \dots & \dots & \vdots \\ \vdots & \vdots & \vdots & \vdots & \vdots \\ R_N & \dots & \dots & \dots & \dots \end{bmatrix} = \begin{bmatrix} I_0 \\ I_1 \\ I_2 \\ \vdots \\ I_N \end{bmatrix} \quad (7)$$

This matrix may be inverted by conventional means to solve for the elemental line source currents.

Once the elemental currents are found for a given injected source current,  $I_s$ , equation (2) may be used to calculate the potential at any point in the source-free region. This potential consists of the contributions from

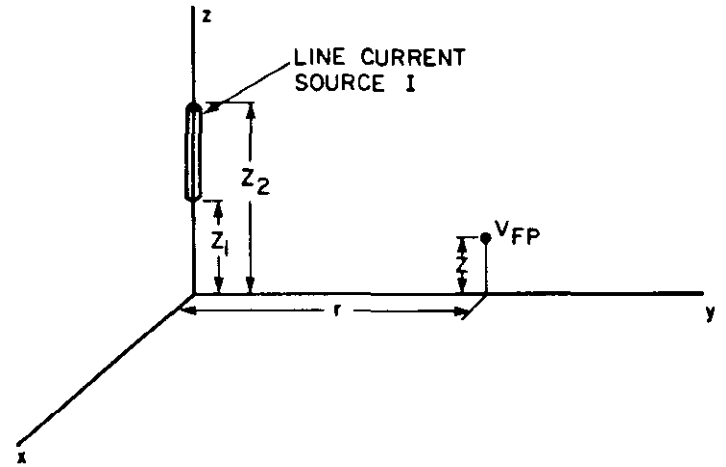


Fig. 5. Relevant dimensions for the calculation of a field point potential due to a line current source.

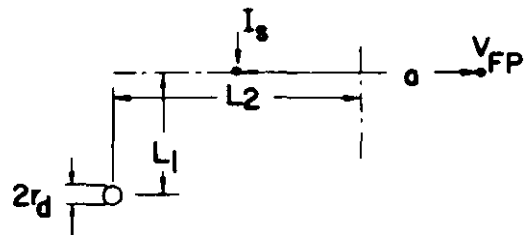


Fig. 6. Plan view of a simple electrode array in the presence of a well casing.

each calculated line source and from the injected current  $I_s$ . Thus

$$V_{FP} = I_0 R_{eF0} + 2I_1 R_{eF1} + 2I_2 R_{eF2} + I_s R_{sF} \quad (8)$$

where

$$R_{eFm} = \frac{\rho}{4\pi \sqrt{r_2^2 + (2ml / M)^2}}$$

and

$$R_{sF} = \frac{\rho}{4\pi a}$$

The normalized apparent resistivity  $\rho_a/\rho$  is then given by

$$\frac{\rho_a}{\rho} = \frac{V_{FP}}{I_s R_{sF}} \quad (9)$$

An example of a  $\rho_a/\rho$  profile for the array geometry of Figure 6 is given in Figure 7.

For a given well casing of finite length, an appropriate choice for the number of elemental line sources,  $M$ , is important. In general, the larger the value of  $M$ , the better the convergence to a final answer. As an example, the solution for a casing 3000 m in length with a current injection point 200 m away will converge to within 1% of a final answer when  $M = 15$  is used. This final answer has been carefully checked by a technique that does not require invoking the reciprocity principle.

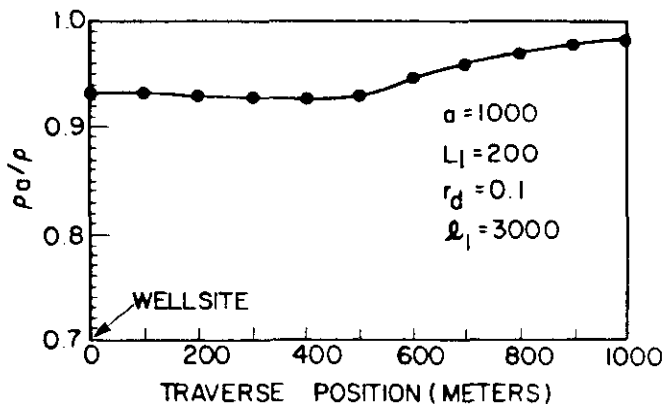


Fig. 7. Apparent resistivity profile obtained by stepping the simple array of Figure 6 past a single well.

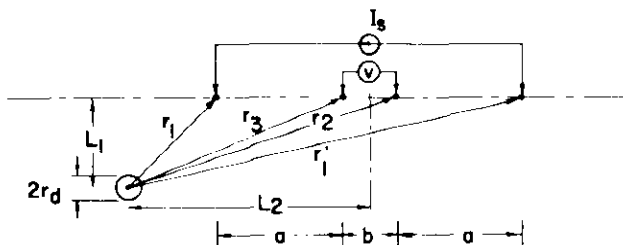


Fig. 8. Plan view of a Schlumberger array and a single well.

EXTENSION TO PRACTICAL MEASUREMENT ARRAYS

The results obtained by using equation (7) can readily be extended to the case of dual-current injection points and dual-potential pickup arrays, such as those encountered in practice, by using the principle of superposition. Typical geometries for the Schlumberger and dipole-dipole arrays are shown in Figures 8 and 9.

Example resistivity profiles for sets of 2, 4 and 6 well casings 7" in diameter and 8000 ft long are shown in Figures 10 and 11, for the Schlumberger and dipole-dipole arrays. The wells are situated at the centres of

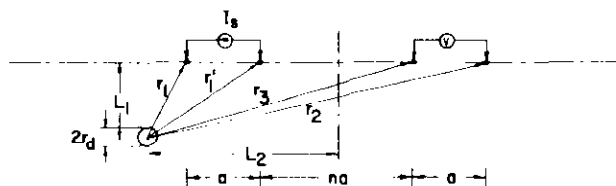


Fig. 9. Plan view of a dipole-dipole array and a single well.

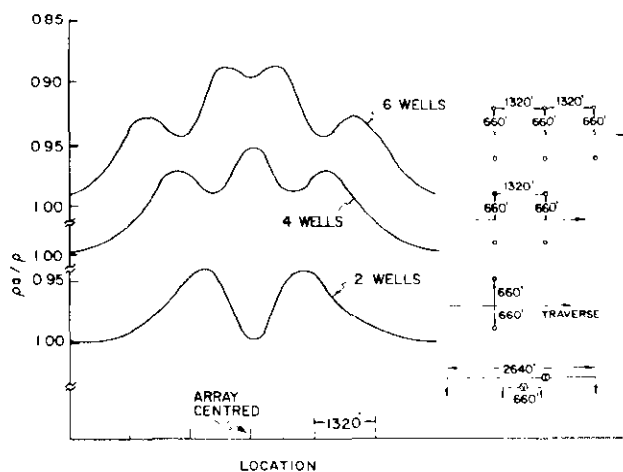


Fig. 10. Theoretical Schlumberger resistivity profiles for sets of 2, 4 and 6 wells on LSD spacings.

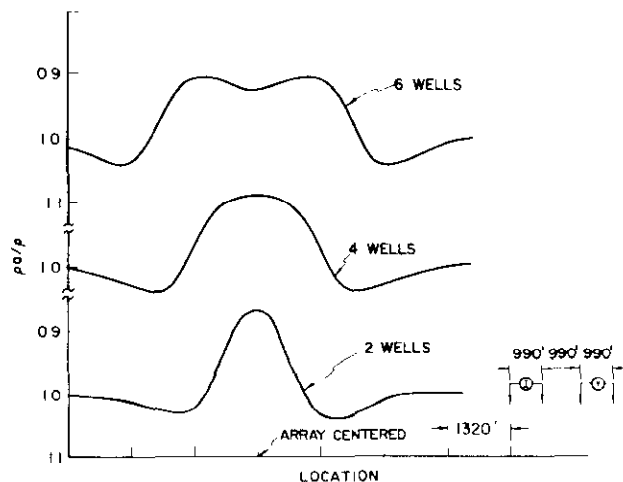


Fig. 11. Theoretical dipole-dipole resistivity profiles for 2, 4 and 6 wells on LSD spacings.

legal subdivisions (LSDs), a situation often encountered in practice. As can be seen, the nature of the profile obtained depends strongly on the well plan, so that no general statement of the shape of an expected profile can be made.

#### INCLUSION OF INTERNAL CASING RESISTANCE AND SURFACE IMPEDANCE

The calculations described above are based on a perfect conductor that is in perfect contact with the surrounding earth. In practice, finite casing resistance and surface impedance, although small, can substantially alter the results obtained on the basis of these assumptions. A casing bulk material resistivity of  $2.5 \times 10^{-7}$  ohm-metres, for example, can reduce the effect of the well casing by as much as a factor of two, because of the redistribution of currents that results in the model as resistance effects are included. Similar effects are obtained for realistic values of surface impedance. A substantial amount of work has been done on these effects and will be described in future publications. However, it can be stated that the results obtained from the simple theory presented here consistently overestimate the effect of the casings.

#### A CASE STUDY

In an attempt to determine whether well casing effects in the field are as theoretically predicted, resistivity profiles were run near a drilling location with and without drill string in the hole. The results are shown in Figure 12. Unfortunately, an exceptionally heavy rain occurred between the two sets of measurements, and a buried fence wire near the traverse caused some small changes in the first stations as shown. Nevertheless, it

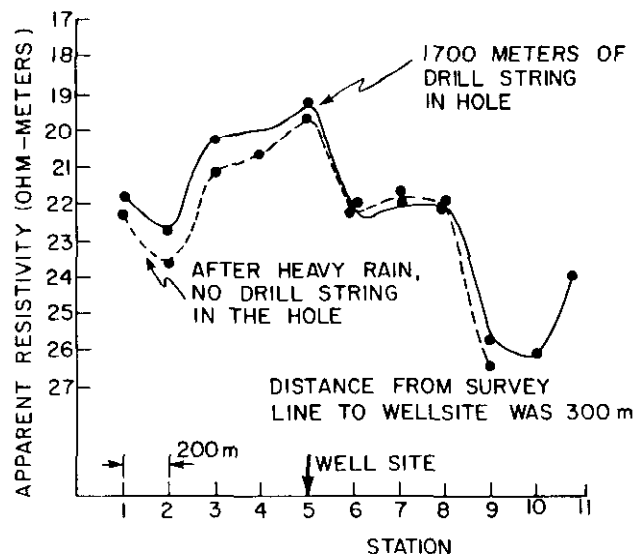


Fig. 12. A case study of the effects of drill string using a Schlumberger array.

is clear that only small differences were seen between the two profiles, as expected theoretically for the geometries involved.

#### MEASUREMENTS OVER KNOWN FIELDS IN ALBERTA

Resistivity profiles were also measured over two large Alberta hydrocarbon reservoirs, as shown in Figures 13 and 14. The measurements were made by using a conventional Schlumberger array, and the resulting resistivity profiles are shown in Figures 15 and 16. Also shown are the subsurface structural profiles, and the theoretical resistivity profiles that would be expected on the basis of well casings only. These theoretical profiles were calculated to include exact details of each well within a half-mile of the traverse, based on data available from well completion records for the fields. In addition, it must be noted that the theoretical profiles are overestimates of the effects of the casings because they do not include casing resistance and surface impedance effects.

In both the Innisfail and Bonnie Glen fields a large residual resistivity anomaly remains after the effects of well casing are removed, suggesting that some effect other than well casing is causing the observed resistivity anomalies.

#### CONCLUSION

An accurate and computationally efficient technique for calculating the effects of well casing on geophysical resistivity surveys has been described. Field measurements over two large hydrocarbon reservoirs in Alberta have been corrected for well casing effects, and a substantial resistivity anomaly remains, suggesting that such anomalies may exist and provide useful exploration input in addition to seismic and other data.

#### REFERENCES

1. Nonseismic Hydrocarbon Exploration Session, 1982, 53rd Annual International S.E.G. meeting, Dallas Convention Centre, Dallas, Texas, Oct. 17-21, p. 471-473.
2. Spies, B.R., 1983, Recent developments in the use of surface electrical methods for oil and gas exploration in the Soviet Union: *Geophysics*, v. 48, p. 1102-1112.
3. Holladay, J.S. and West, G.F., 1984, Effect of well casings on electrical surveys: *Geophysics*, v. 49, p. 177-188.
4. Klein, J.D., 1983, Spectral induced polarization survey, David Field, Alberta, Canada: Presented at the 36th Annual Meeting of the Midwest Society of Exploration Geophysicists, Denver, Colorado, March 6-9.
5. Johnston, R.H., Trofimenkoff, F.N. and Haslett, J.W., 1984, Electromagnetic reflection from subsurface high resistivity anomalies: Presented at the National Convention of the Canadian Society of Petroleum Geologists and Exploration Geophysicists, Calgary, Alberta.
6. Trofimenkoff, F.N., Johnston, R.H., Haslett, J.W. and Watt, J.T., 1984, Image theory analysis of fields due to a step in the current in a long line on the surface of the earth: *IEEE Trans. Geoscience and Remote Sensing*, v. GE-22, p. 155-159.

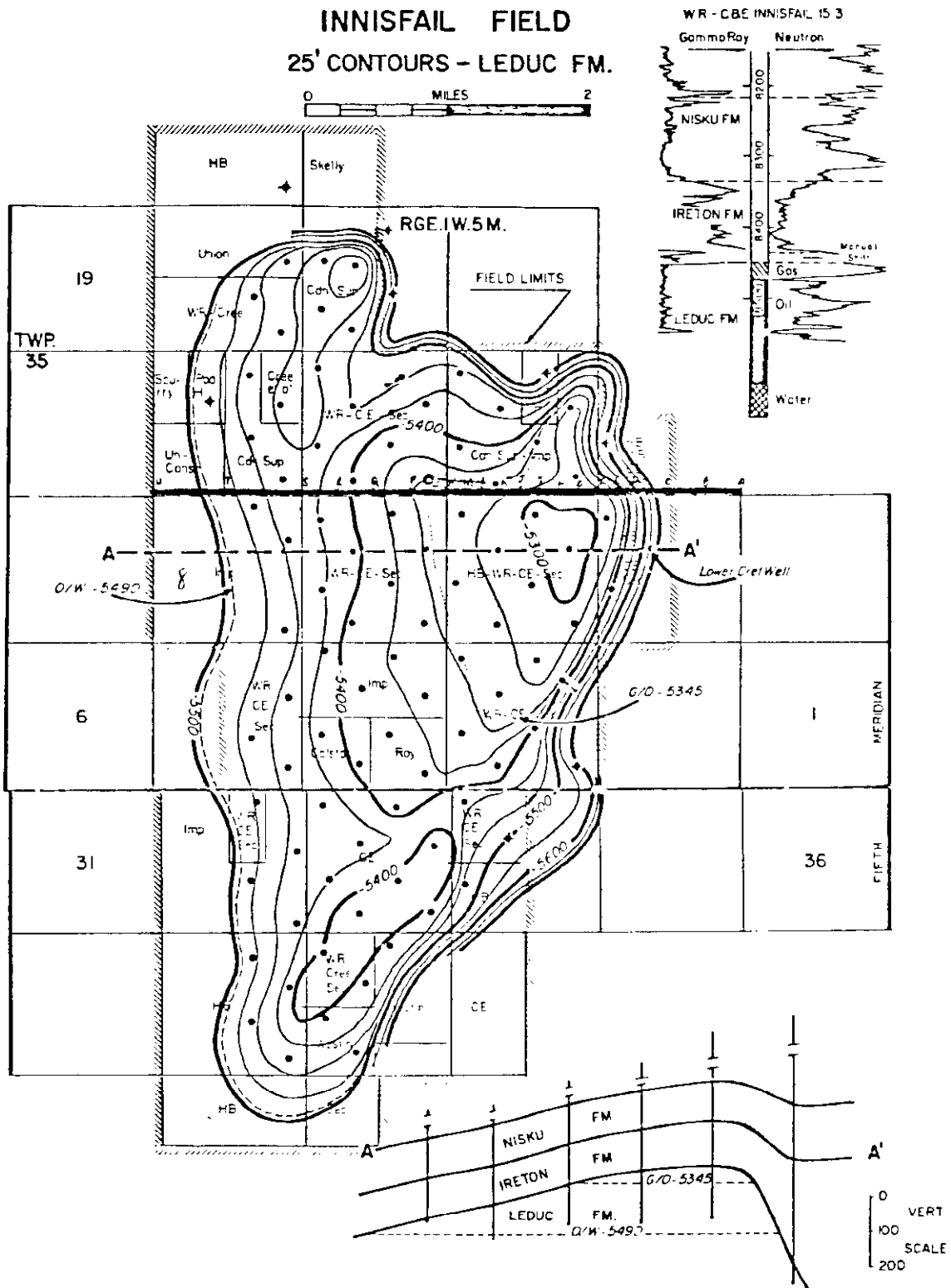


Fig. 13. Innisfail field<sup>10</sup>.

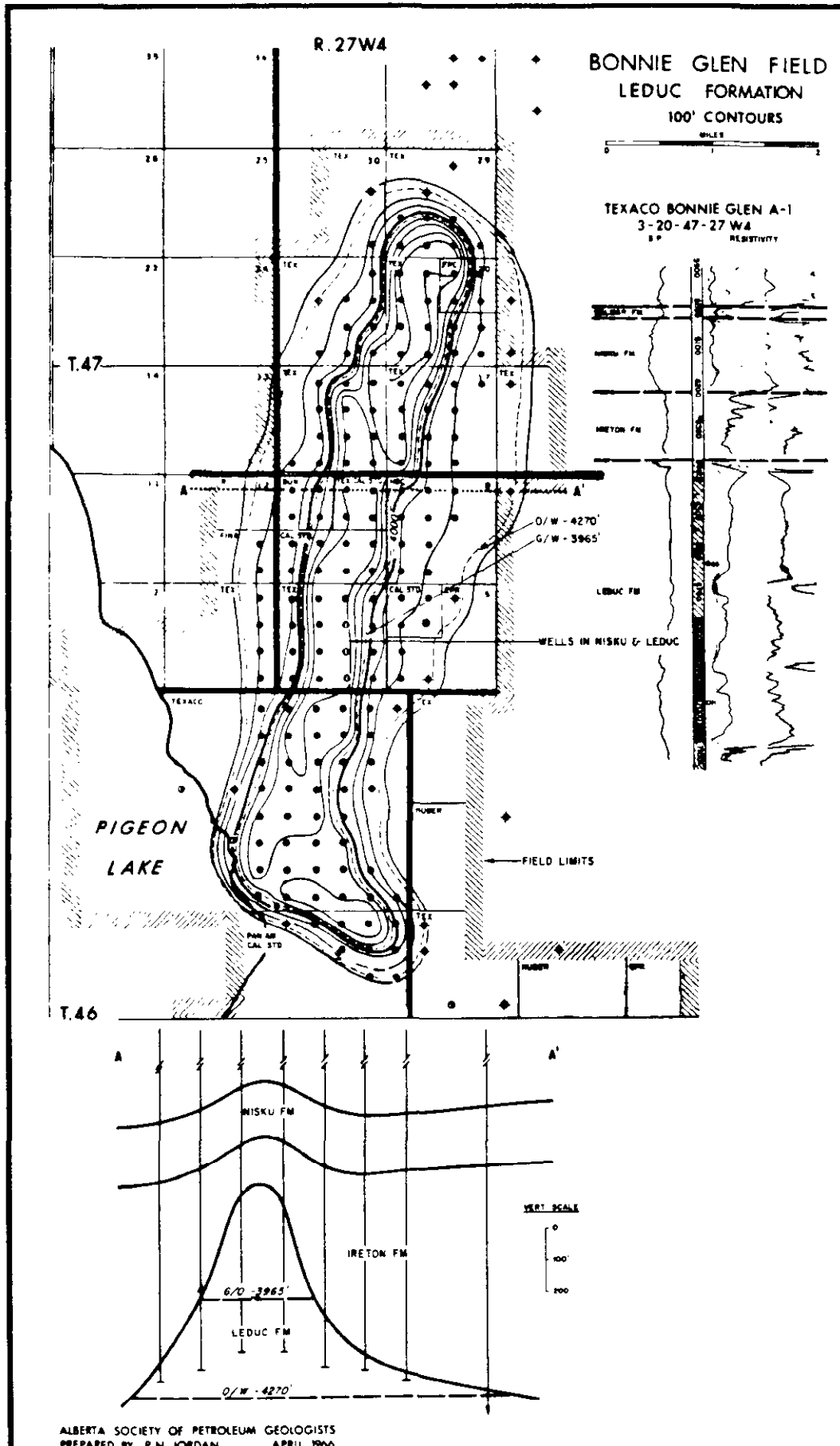


Fig. 14. Bonnie Glen field<sup>11</sup>.

7. ———, Johnston, R.H. and Haslett, J.W., 1982. Electromagnetic coupling between parallel lines on a uniform earth: *IEEE Trans. Geoscience and Remote Sensing*, v. GE-20, p. 197-200.
8. Bhagwan, J. and Trofimenkoff, E.N., 1982. Electric drill stem telemetry: *IEEE Trans. Geoscience and Remote Sensing*, v. GE-20, p. 193-197.
9. Wait, J.R., 1983. Resistivity response of a homogeneous earth with a contained vertical conductor: *IEEE Trans. Geoscience and Remote Sensing*, v. GE-21, p. 109-113.
10. White, R.J., 1960. Innisfail Field. *In: Oil Fields of Alberta*; Calgary, Alberta Society of Petroleum Geologists, p. 136-137.
11. Jordan, P.N., 1969. Bonnie Glen Field. *In: Gas Fields of Alberta*; Calgary, Alberta Society of Petroleum Geologists, p. 70-71.

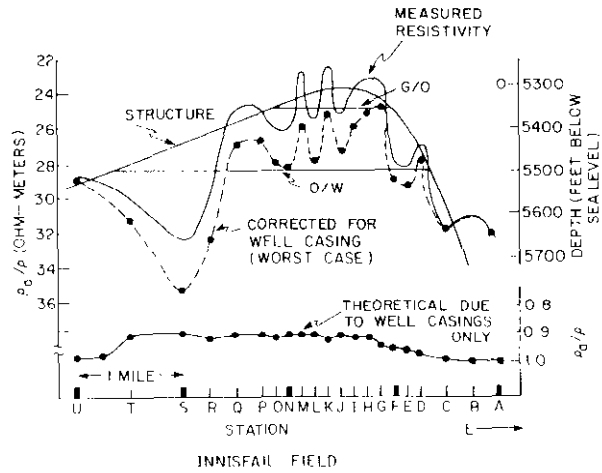


Fig. 15. Raw and corrected apparent resistivities compared with subsurface structure for the Innisfail field.

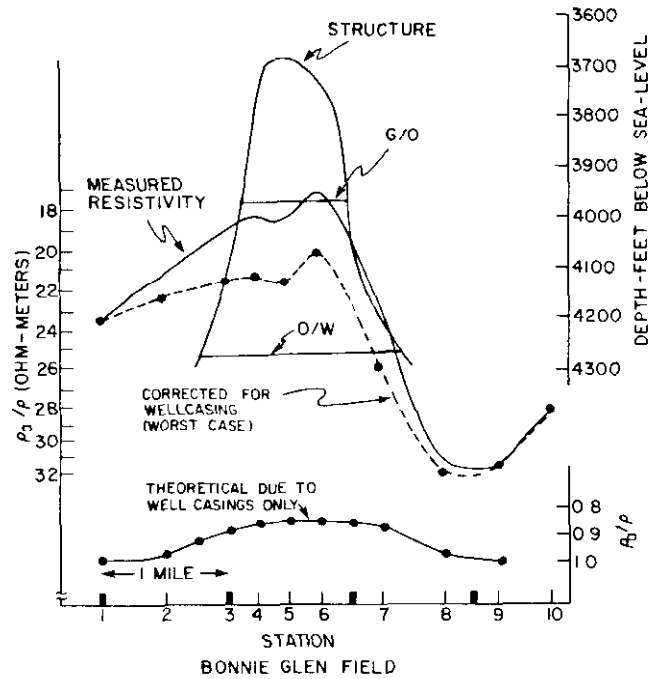


Fig. 16. Raw and corrected apparent resistivities compared with subsurface structure for the Bonnie Glen field.